# Single - Channel Multi - Coil Array

**I. Muradyan[1], F. Zhou[2], P. Soni[2], M. Dabaghyan[1], S. Patz[1], and M. I. Hrovat[3]**
[1]Department of Radiology, Brigham and Women's Hospital, Boston, MA, United States, [2]University of Massachusetts, Lowell, [3]Mirtech, Inc, Brockton, MA, United States

## Introduction

The separation of Gray and White Matter perfusion is still a challenging problem although several techniques are available for the task: autoradiography, PET, CT, Arterial Spin Labeling MRI. However, the values they provide disagree not only between different modalities, but even within the same one (1). As of now, even the GM/WM perfusion ratio is not determined within an acceptable error margin. Xe MRI has the potential to shed more light on the process and help differentiate GM and WM perfusion. Due to its large electron cloud, the Xe spectrum in the brain has easily distinguishable peaks corresponding to Xe dissolved in GM and WM (2-4).

Although a volume coil provides a more homogeneous B1 field compared to a surface coil, it has the disadvantage of exciting HP Xe while it is still in transit to the brain tissue, depleting available magnetization before it reaches the tissue of interest and decreasing SNR. To prevent this loss we propose use of a multi-transceiver coil array.

## Materials and Methods

The single channel multi-coil array allows one to have multiple transceiver (transmit/receive) coils with only a single RF channel. Even though many present-day MR scanners support multiple receiver channels, only a relatively few scanners support multiple transmit channels.

We constructed a 4 coil transceiver array where each coil has a diameter of 10cm. The transceiver coils were designed to minimize pin-diode losses and operate as efficiently as a single transmit/receive coil without pin diodes. The coils are connected to the 4-port rf switch (see Figure 1). The transmit/receive switch upon receiving a pin-diode control signal from the scanner, passes it on to the TTL logic witch then toggles the outputs of the rf switch. The logic determines which transceiver coil should be active for this particular pulse, and activates the corresponding channel on the RF switch. A particular coil is thus selected for both transmit and receive modes. For the next pulse the cycle is repeated, only this time it might be a different coil that is activated.

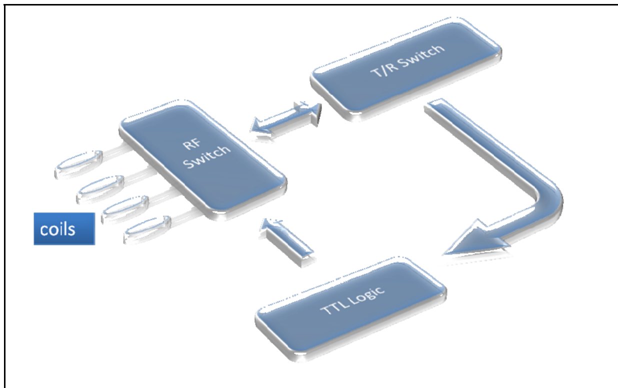


Figure 1. Schematic of the single-channel multi-coil array.
T/R switch passes atrigger to the TTL logic, which turns one of the channels on the rf switch on, thus activating one of the coils for transmit/receive.

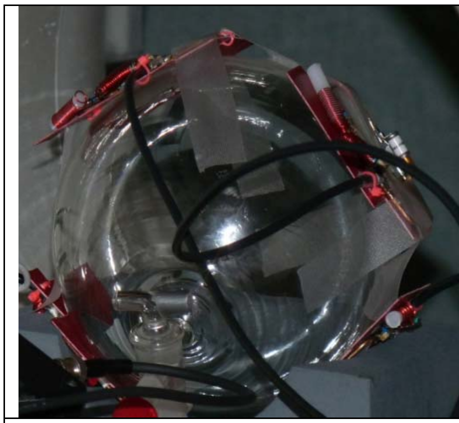

Figure 2. 1L HP Xe cell inside the coil array.

Although there are only 4 channels on the RF Switch, the TTL logic is currently designed to support up to 16 coils. Also, the logic is designed such that it supports up to 16 pulses applied to any of the channels before switching to the next coil. In other words, it would be possible to set up a case, when 16 successive RF pulses are applied to the same coil before the channel is switched to a different one.

The array is tuned to Xe frequency at 2.89T. A number of calibration studies of the coils were done using several xenon phantoms. Experiments were performed on a Siemens Tim Trio scanner with multinuclear imaging capability, located at Martinos Center for Biomedical Research, Charlestown, MA. Figure 2 shows an experimental setup when hyperpolarized xenon gas is thawed into a 1L glass cell and placed inside the coil array (Figure 2). The coils of the array are distributed around the periphery of the cell, and the TTL logic is setup such that for each consecutive rf pulse the selected coil is incremented. Thus, for the 1$^{st}$ shot coil #1 will be active, for the 2$^{nd}$ shot – coil #2, etc. and coils #1 will activate again for shot #5. Three 3D low resolution (16x16x10) gradient echo images were collected without a delay to calculate the flip angle map of the coils.

The raw data were analyzed in Matlab. Gas images were reconstructed and then masked by 5% of maximum intensity value, i.e. all pixels that had less than 5% of the max. signal were set to Not-a-Number. The data was then fit to $S_n = S_1 \cdot \cos^{(n-1)N}(\alpha)$ in a pixel-by-pixel manner. Here *n* is the image number, *N* is the number of rf pulses applied per image per coil and *α* is the flip angle. In this model we neglect the T1 decay of the signal, since image acquisition time is much shorter than T1 of the gas in a glass cell (1s vs. 1hr).

## Results

Figure 3 shows the images acquired for each of the coils separately (a), the combined image (b) and the calculated flip angle map (c). The flip angle values vary from 5 degrees (dark blue in the middle of the cell) to 30 degrees (dark red on the periphery). The diameter of the cell is about 12 cm, hence about 2 cm from each side sees a flip angle of ~ 20 ± 5 degrees, which is in an agreement with predicted flip angle (25 deg).

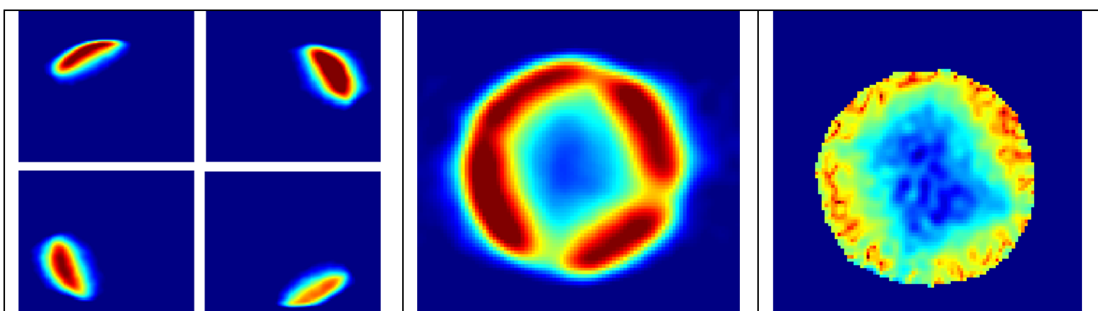

Figure 3 (a) 1L gas cell phantom of HP Xe. Images are from 4 coils of the array.

Figure 3 (b) Combined Image from all 4 coils

Figure 3 (c) Flip angle map obtained from fitting the data to the above equation.

## Discussion

This type of single-channel multi-coil array provides the capability to perform multi-coil imaging on single channel scanners. One of the most suitable applications for this type of an array is cerebral perfusion imaging with hyperpolarized xenon. The use of the array would ensure that xenon polarization is not depleted unless the coil in that region is activated. Also, by construction, this system provides certain localization of the measured signal even in the case of a simple spectroscopic measurement: the coils are sufficiently separated from each other to ensure that signal collected by one of the coils is originated from a particular region, and no signal from other regions will leak in.

**Acknowledgement:** The study is supported by Brigham and Women's Hospital, Department of Radiology BRREF grant, Mirtech, Inc, and Martinos Center for Biomedical Research (NCRR grant #P41RR14075).

**References:** (1) Van Gelderen et.al. MRM 59 (2008) 788-795; (2) Kilian et al., MRM 51 (2004) 843-847; (3) Choquet et al., MRM 49 (2003) 1014-1018; (4) Nakamura et al., MRM 53 (2005) 528-534